Comparison between filter- and optimization-based motion cueing algorithms for driving simulation

Cleij, D.; Venrooij, J.; Pretto, P; Katliar, M.; Bülthoff, Heinrich H.; Steffen, D.; Hoffmeyer, F. W.; Schöner, H. P.

DOI
10.1016/j.trf.2017.04.005

Publication date
2019

Document Version
Final published version

Published in
Transportation Research. Part F: Traffic Psychology and Behaviour

Citation (APA)
Cleij, D., Venrooij, J., Pretto, P., Katliar, M., Bülthoff, H. H., Steffen, D., Hoffmeyer, F. W., & Schöner, H. P. (2019). Comparison between filter- and optimization-based motion cueing algorithms for driving simulation. *Transportation Research. Part F: Traffic Psychology and Behaviour*, *61*, 53-68. https://doi.org/10.1016/j.trf.2017.04.005

Transportation Research Part F 61 (2019) 53–68

Contents lists available at ScienceDirect

Transportation Research Part F

journal homepage: www.elsevier.com/locate/trf

Comparison between filter- and optimization-based motion cueing algorithms for driving simulation

D. Cleij [a,*], J. Venrooij [a], P. Pretto [a], M. Katliar [a], H.H. Bülthoff [a], D. Steffen [b], F.W. Hoffmeyer [b], H.-P. Schöner [b]

[a] Max Planck Institute for Biological Cybernetics, Tübingen, Germany
[b] Daimler AG, Driving Simulators Dept. RD/FFS, Sindelfingen, Germany

ARTICLE INFO

Article history:
Received 29 December 2016
Accepted 10 April 2017
Available online 24 May 2017

Keywords:
Motion cueing
Optimization-based
Filter-based
Continuous rating

ABSTRACT

This paper describes a driving simulation experiment, executed on the Daimler Driving Simulator (DDS), in which a filter-based and an optimization-based motion cueing algorithm (MCA) were compared using a newly developed motion cueing quality rating method. The goal of the comparison was to investigate whether optimization-based MCAs have, compared to filter-based approaches, the potential to improve the quality of motion simulations. The paper describes the two algorithms, discusses their strengths and weaknesses and describes the experimental methods and results. The MCAs were compared in an experiment where 18 participants rated the perceived motion mismatch, i.e., the perceived mismatch between the motion felt in the simulator and the motion one would expect from a drive in a real car. The results show that the quality of the motion cueing was rated better for the optimization-based MCA than for the filter-based MCA, indicating that there exists a potential to improve the quality of the motion simulation with optimization-based methods. Furthermore, it was shown that the rating method provides reliable and repeatable results within and between participants, which further establishes the utility of the method.

1. Introduction

Motion cueing is the process of converting a desired physical motion, obtained from, e.g., a vehicle model, into motion simulator input commands. This conversion is done by a motion cueing algorithm (MCA). In past decades, many different types of MCAs have been introduced (Garrett, Best, & Loughborough, 2010). The vast majority of them are variations of the filter-based approach, which relies mainly on scaling down and filtering the physical motions such that the commanded motion lies within the limited motion envelope of a simulator.

Recently, several optimization-based MCAs have been developed, e.g. (Mayrhofer et al., 2007; Beghi, Bruschetta, Maran, 2012; Garrett & Best, 2013; Venrooij et al., 2015). The most important difference with filter-based approaches is that an optimization-based MCA produces an optimized output, in which simulator constraints are explicitly accounted for, instead of a filtered output for which it is not guaranteed it lies within the simulator's operational capabilities. In some optimization-

* Corresponding author.
E-mail addresses: diane.cleij@tuebingen.mpg.de (D. Cleij), joost.venrooij@tuebingen.mpg.de (J. Venrooij), paolo.pretto@tuebingen.mpg.de (P. Pretto), mikhail.katliar@tuebingen.mpg.de (M. Katliar), heinrich.buelthoff@tuebingen.mpg.de (H.H. Bülthoff), dennis.steffen@daimler.com (D. Steffen), friedrich.hoffmeyer@daimler.com (F.W. Hoffmeyer), hans-peter.schoener@daimler.com (H.-P. Schöner).

http://dx.doi.org/10.1016/j.trf.2017.04.005
1369-8478/

based MCAs the motions of the simulator platform are optimized which are then converted to simulator control commands by low-level controllers, e.g., (Mayrhofer et al., 2007; Beghi et al., 2012). In others, the simulator control commands are optimized directly, e.g., (Garrett & Best, 2013; Venrooij et al., 2015).

It is clear that filter-based and optimization-based MCAs are fundamentally *different* algorithms, but it is not readily apparent which provides *better* motion cueing, if at all, and under which conditions. One can compare the algorithms' output, i.e., the commanded simulator motions, but that does not provide a direct answer to the question how the motion cueing quality of the algorithms is actually *perceived* by simulator occupants. The study presented in this paper aimed at providing some answers to that question by performing an experimental comparison.

The filter-based and optimization-based motion cueing approaches were compared in a driving simulation experiment, executed on the Daimler Driving Simulator (DDS) of Daimler AG in Sindelfingen, Germany. In the experiment, an optimization-based algorithm, developed by the Max Planck Institute for Biological Cybernetics in Tübingen, was compared against Daimler's filter-based MCA, using a newly developed motion cueing quality rating method (Cleij et al., 2015). The two algorithms will be referred to, in this paper, as MCA_{OPT} and MCA_{FIL} respectively. The goal of the comparison is to investigate whether optimization-based MCAs have, compared to filter-based approaches, the potential to further improve the quality of motion simulations.

2. Motion cueing algorithms

2.1. Filter-based motion cueing

Filter-based motion cueing algorithms consist of a combination of gains and filters, which transform (desired) vehicle motion into simulator set-points in real-time. Typically, the filters have a high-pass characteristic to prevent low-frequency accelerations from consuming a considerable part of the simulator's motion space. The gain functions can be linear or nonlinear and are adjustable, with the aim of reaching a good motion representation in a wide range of manoeuvres, preferably with a constant set of parameters. Special requirements of the manoeuvre that is to be simulated, like tight curves or turns, might be considered separately by the algorithm in order to provide good motion cueing quality while keeping the simulator within its operational limits. Well-known characteristics of the filter-based approach are tilt-coordination (where low-frequency components of the linear acceleration are reproduced by tilting the simulator platform) and motion washout (the ever-present push to return to the initial position). Such MCAs are commonly referred to as washout filters.

The MCA_{FIL} for non-professional driver applications is based on a classical washout algorithm. Scaling factors and filters are used in all six degrees of freedom (DOF) to calculate the motion cues. Lateral, vertical and yaw excitations are dynamically limited by high-pass filters. A modified tilt-coordination algorithm provides an impression of steady-state acceleration in longitudinal direction and maximizes the use of the linear rail.

The main goal of the MCA_{FIL} is to provide linear motion cues within the envelope of the motion system even during worst-case manoeuvres. The algorithm takes the outputs of the vehicle simulation (accelerations and rotation angles and rates in 6 DOF) and calculates the commands for the motion system at 500 Hz. When used in driver-in-the-loop studies, the algorithm operates in real-time such that the driver is free to choose velocity, acceleration, deceleration and manoeuvres like lane change or overtaking other cars.

2.2. Optimization-based motion cueing

Optimization-based motion cueing optimizes simulator motions or control commands through an optimization algorithm. An often-used approach is Model Predictive Control (MPC). MPC is a control methodology that optimizes the current control signal based on a process model and a future reference trajectory of finite length, while taking constraints into account (Rawlings & Design, 2015). The optimization is governed by an objective function which quantifies the difference between (desired) vehicle motion and simulator motion. The optimization is constrained by the simulator's actuator limits. As a result, the optimized simulator control inputs and states always lie within the simulator's operational capabilities. MPC-based algorithms utilize predictions of future reference signals, using a 'prediction horizon' of a certain length, to compute the current control action. The advantage of this is that the current control action is optimized while taking future simulator states and control actions into account (Maran et al., 2015).

In general, an MPC-based MCA finds a sequence of controls $\boldsymbol{u}$ and states $\boldsymbol{x}$ which minimizes the following objective function:

$$J(\boldsymbol{x},\boldsymbol{u}) = \sum_{k=1}^{N}\left(\|\boldsymbol{u}_k\|_P^2 + \frac{1}{2}\left(\|\boldsymbol{y}(\boldsymbol{x}_k,\boldsymbol{u}_k) - \widehat{\boldsymbol{y}}_k\|_R^2 + \|\boldsymbol{y}(\boldsymbol{x}_{k+1},\boldsymbol{u}_k) - \widehat{\boldsymbol{y}}_{k+1}\|_R^2\right)\right) + \sum_{k=1}^{N+1}\|\boldsymbol{x}_k - \boldsymbol{x}_0\|_Q^2 \tag{1}$$

Subject to the constraints:

$$\begin{aligned} &\boldsymbol{x}_{k+1} - F(\boldsymbol{x}_k,\boldsymbol{u}_k) = 0 \\ &\boldsymbol{u}_{min} \leqslant \boldsymbol{u}_k \leqslant \boldsymbol{u}_{max} \\ &\boldsymbol{x}_{min} \leqslant \boldsymbol{x}_k \leqslant \boldsymbol{x}_{max} \end{aligned} \tag{2}$$

where N – number of time steps, $\boldsymbol{x}_0$ – the "neutral" state of the simulator, $\boldsymbol{y}(\boldsymbol{x}_k, \boldsymbol{u}_k)$ – inertial signal at the head point in the simulator as a function of its state and input, – inertial signal at the head point in the vehicle (reference value), P, Q, R – symmetric positive-definite weighting matrices for penalizing control input, deviation from the neutral state and error in the inertial signal, respectively. F is the function that describes discrete-time dynamics of the system, $\boldsymbol{u}_{min}$, $\boldsymbol{u}_{max}$, are the lower and upper bounds of the inputs and states. The inertial signal is defined as

$$\boldsymbol{y} = \begin{bmatrix} \boldsymbol{f} \\ \boldsymbol{\omega} \end{bmatrix} \tag{3}$$

where $\boldsymbol{f}$ – specific force, ω – rotational velocity at the head point.

The MCA_{OPT} is described in more detail in (Venrooij et al., 2015; Pretto, Venrooij, Nesti & Bülthoff, 2015). For the experiment described in this paper the process model was adjusted to incorporate and cope with the parallel, rather than serial, model of the Daimler simulator. In the current paper, a *trajectory-based* optimization was performed, which means that the information of the entire trajectory was provided to the algorithm at the start of the optimization: i.e. in Eq. (1), is the total number of trajectory samples and is obtained from a recording of the manoeuvre that was to be simulated (instead of a prediction of the future reference). In theory, this should lead to the best cueing quality, as the maximum amount of available information (i.e., a 'perfect prediction') is provided to the optimization algorithm. A clear disadvantage of this approach is that it makes the algorithm only suitable for simulation of pre-recorded manoeuvres. It is possible to use prediction methods to obtain real-time predictions of the future reference signal, which makes the algorithm suitable for driver-in-the-loop simulations, e.g., (Beghi et al., 2012). It is to be expected that this would result in a lower simulation quality compared to the trajectory-based optimization approach used in the current study (Katliar et al., 2015).

The weighting matrices used in the objective function are: $P = 0.1$, $Q = 0$, $R = \mathrm{diag}(1, 1, 1, 10, 10, 10)^2$. As the value for Q was zero, there was no penalty for deviation from the neutral state, which implies that the algorithm did not exhibit washout behaviour. The weighting factor 10 for the rotational velocities is chosen as an approximate ratio of standard deviation of specific force components in m/s^2 and standard deviation of rotational velocity components in rad/s for typical car manoeuvres.

The optimization was constrained by the actuator limits. For safety reasons, the bounds were set at 95% of the actual position, velocity and acceleration limits of each actuator. In addition, the simulator state was constrained by the condition that the initial and final position of the simulator should be upright (zero degrees of roll, pitch and yaw) and the initial and final velocity of simulator should be zero. The optimization was performed using CasADi toolbox (Anderson, 2013) and Ipopt solver (Wächter & Biegler, 2006).

2.3. Algorithm comparison

It is important to note that the two MCAs described above are very different algorithms, each with their own characteristics, see Table 1.

The MCA_{FIL} is a robust, real-time algorithm, suitable for driver-in-the-loop simulations. The MCA_{OPT} performs its optimization based on perfect knowledge of the entire driving manoeuvre, making it unsuitable for real-time driver-in-the-loop applications, but suitable for passive simulations.

The MCA_{OPT} does not run in real-time due to the high computational load associated with the optimization. The optimization of the trajectory used in this study – with a duration of approximately 5 min – took a few hours on a regular PC. After the optimization, the output of the MCA_{OPT}, which provided data at a sampling rate of 50 Hz, was resampled (interpolated) to 500 Hz, in order to run synchronously with the output of the MCA_{FIL}.

During the optimization, the MCA_{OPT} utilized exact knowledge on the desired motion for all future time steps (trajectory-based optimization). Such an optimization would not be possible if the knowledge about the future is limited, as is the case in real-time driving scenarios with a driver in the loop. In that case, prediction algorithms would be required to obtain an estimate of the future reference trajectory. The effect of using (different approaches to) real-time prediction on simulation quality remains a topic to be addressed in future studies.

Table 1
Comparison of algorithm characteristics.

	MCA_{FIL}	MCA_{OPT}
Type	Filter-based	Optimization-based
Real-time capable	Yes	No
Driver-in-the-loop applications	Suitable	Not suitable
Sampling rate	500 Hz	50 Hz
Future reference	Not applicable	Entire trajectory
Accounting for simulator limits	Through manual tuning	Through constrained optimization
Tuned	Yes	No

Furthermore, the optimization of the MCA_{OPT} is constrained by the simulator's actuator limits. As a result, the optimized simulator control inputs and states always lie within the simulator's operational capabilities. This is not guaranteed for the output of the MCA_{FIL}, where simulator limits are typically accounted for by tuning the algorithm's parameters. The MCA_{OPT} did not need tuning for the experiment described in this paper. The implementation of the MCA_{OPT} used in the current study did not account for perceptual factors like drivers' motion sensitivity and thresholds (Pretto et al., 2015). It is to be assumed that the implementation of such features will further improve the cueing quality of the MCA_{OPT}.

Due to the above differences, this study is not to be considered as a competitive comparison between MCA alternatives, but rather as an attempt to gain insight in the potential that an optimization-based approach has to offer with respect to well-established filter-based approaches.

3. Methods

3.1. Research questions

The primary research question of this study is whether optimization-based MCAs have the potential to further improve the quality of motion simulations compared to filter-based approaches. At the start of the study it was unknown whether there would be any measurable differences between the two algorithms, and if so, what can be learnt from these differences to further improve motion cueing.

In order to measure the quality of the motion cueing, a quality rating method developed at the Max Planck Institute for Biological Cybernetics in Tübingen was utilized. The method was described and evaluated in (Cleij et al., 2015). As the rating method was only recently developed, a secondary research question was whether the method provides reliable and repeatable results within and between participants.

3.2. Apparatus

The experiment was conducted in the Daimler Driving Simulator (DDS), an electrical hexapod platform mounted on a 12 m long linear axis (Zeeb, 2012) (Fig. 1, left). For this experiment, the car's longitudinal axis was aligned with the simulator's linear axis by rotating the cabin in the dome (Fig. 1, right). This adjustment provides a relatively large motion space for the reproduction of longitudinal accelerations and deceleration with the disadvantage that the space for lateral motion is limited. The driver's cabin was a standard Mercedes-Benz C-Class model (W204) equipped with an additional display showing the rating bar (described below).

3.3. Participants

In total 18 participants, 9 females, aged between 21 and 40 (mean = 29.3; std = 5.7) took part in the experiment. All had previous experience in driving simulators, but no or limited knowledge of motion cueing. They were expert drivers with a minimum mileage of 10,000 km per year (mean = 17,222; std = 7496). Two participants did not complete the experiment due to motion sickness symptoms and their data were excluded from the analysis.

3.4. Experimental procedure

In the experiment, participants were presented with four pairs of evaluation trials, of which the first pair was used for training purposes. Each trial consisted of the playback of an identical pre-recorded simulated drive. While the visuals remained unaltered, the vehicle motions of the simulated drive were processed by either the MCA_{FIL} or the MCA_{OPT}, generating two different simulator trajectories. These trajectories were repeatedly presented in random order at each trial pair. In total, participants rated each trajectory four times, of which the last three were included in the data analysis. During the playback, the participants did not need to take any actions on the steering wheel or pedals. Instead, they were asked to concentrate on the movements of the simulator and rate the perceived motion mismatch, i.e., the perceived mismatch between the motion felt in the simulator and the motion one would expect from a drive in a real car. The experiment lasted approximately 1 h, of which 45 min in the DDS (Table 2).

3.5. Rating procedure

The ratings were provided using the built-in rotary COMAND-knob of a Mercedes C-Class. By rotating it, participants controlled a rating bar with 15 coloured markers, visible on a small screen located to the left of the steering wheel (Fig. 2). A rotation to the left reduced the number of visible marks (lower motion mismatch); a rotation to the right increased the number of visible marks (higher motion mismatch). There was always at least one green mark visible. The quality of the motion cueing was rated in two ways:

A continuous rating (CR) method was used to measure time-varying aspects of the perceived mismatch between real and simulated drive. For the CR, participants were asked to continuously assign a value (magnitude) to the instantaneous per-

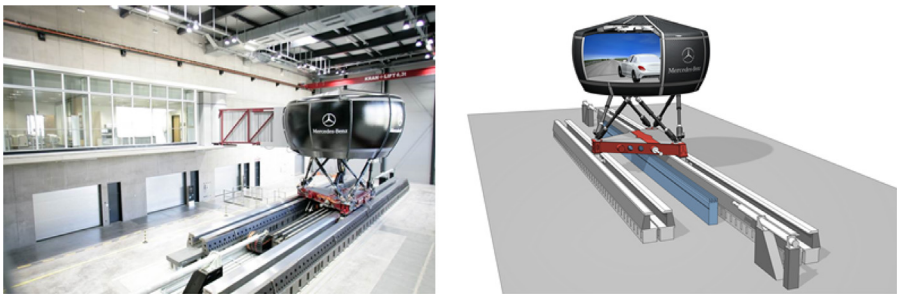

Fig. 1. Exterior of the Daimler Driving Simulator (DDS) (left) and the car orientation during the experiment (right).

Table 2
Overview of experiment procedure.

TRAINING (1 trial pair, 10 min)	Familiarization with rating device and procedure
EXPERIMENT PART 1 (1 trial pair, 10 min)	Motion mismatch rating: CR followed by OR for each trial
BREAK (5 min)	
EXPERIMENT PART 2 (2 trial pairs, 20 min)	Motion mismatch rating: CR followed by OR for each trial

Fig. 2. Location of rating bar and rating knob in the car cabin. The rating bar has 15 coloured marks, where green/red marks indicated low/high perceived mismatch. (For interpretation of the references to colour in this figure legend, the reader is referred to the web version of this article.)

ceived motion mismatch via the rotary knob during the playback. If no mismatch was perceived they were asked to provide a rating of zero.

After each trial the participants were asked to provide an overall rating (OR), by indicating the perceived motion mismatch of the entire playback. The OR resulted in a single rating for each trial.

The rating method is described in more detail in (Cleij et al., 2015).

3.6. Stimuli

The recorded simulated drive that was used in this experiment was performed by a human driver. The drive consisted of different manoeuvres combined into one realistic drive in both rural and city surroundings of about 5 min. The chronological list of manoeuvres that occurred during the drive is shown below.

- InitAcc: initial mild acceleration along a rural road up to the speed of 100 km/h.
- RuralCurves: drive over a rural road consisting of a large-radius left, right and left curve, during which a constant speed was maintained.
- OverTake: double lane change manoeuvre at constant speed to avoid a car parked on the right-hand side of the road.

- SlowDown50: upon entering an urban area the speed is initially reduced from 100 to 70 km/h and then from 70 to 50 km/h.
- TrafLightDec: driving through a gentle curve and decelerating to a full stop in front of a red traffic light.
- TrafLightWait: standing still in front of the red traffic light for ~6 s.
- TrafLightAcc: accelerating from the full stop to 50 km/h after the traffic light switched to green.
- City1: multiple gentle curves through the city at a constant speed of 50 km/h.
- Roundabout: decelerating to 20 km/h, driving through a four-exit roundabout, exiting at the second exit and accelerating back to 50 km/h.
- City2: multiple curves through the city at a constant speed of 50 km/h.
- TurnLeft: decelerating to 20 km/h, driving through a 90° left turn and accelerating back to 50 km/h.
- City3: multiple gentle curves through the city at a constant speed of 50 km/h.
- FinalDec: deceleration to a full stop at a red traffic light.

4. Results

To compare the two MCAs, first the results and reliability of the overall and continuous ratings are shown in Section 4.1. To determine which parts of the drive are responsible for these differences, the continuous rating is analysed per manoeuvre in Section 4.2. In Section 4.3 a comparison between the continuous rating and the motion cueing errors over this time interval is shown as an indication of what caused the perceived mismatch during these manoeuvres. To minimize the cueing errors, both MCAs made use of different cueing mechanisms which are described in Section 4.4. Finally in Section 4.5 the implementation of these mechanisms to generate the linear acceleration in the driver frame of reference in the Daimler Driving Simulator is explained.

4.1. Rating results and reliability

Using the method described above, participants rated the perceived motion mismatch between 0 (no motion mismatch) and 14 (strong motion mismatch). Note that a higher rating value implies a lower cueing quality.

To test for significant differences between mean ratings the parametrized paired t-test (test statistic = t) and repeated measures ANOVA (test statistic = F) were used. Because the mean ratings were not always normally distributed, the Lilliefors test for normality and generalized ESD (extreme Studentized deviate) test were used to check the normality and outlier assumptions of these tests. If these tests were not passed, the non-parametric Wilcoxon signed-rank test (test statistic = z) and the Friedman test (test statistic = χ^2) were used instead of the paired t-test and ANOVA respectively.

The average results obtained for the overall rating (OR) are shown in Fig. 3. The mean overall rating (MCA_{FIL} = 7.0, MCA_{OPT} = 3.0) across all participants differs significantly between MCAs: $z = 3.2154$, $p < 0.01$. This indicates that participants felt less motion mismatch with the MCA_{OPT} than with the MCA_{FIL}. The overall rating does not change significantly for either of the MCAs over the three evaluation trials (MCA_{FIL}: $F(47) = 0.91123$, $p > 0.05$, MCA_{OPT}: $\chi^2(47) = 2.4615$, $p > 0.05$).

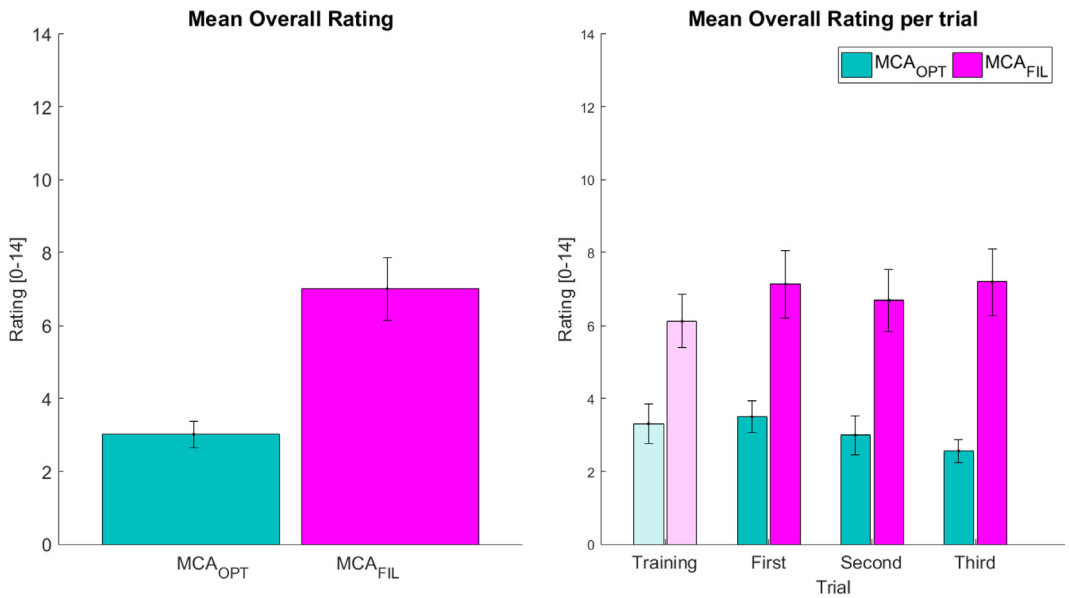

Fig. 3. Mean overall rating across three evaluation trials (left) and mean overall rating per trial (right). Error bars indicate the standard error.

The average results obtained for the continuous rating (CR) are shown in Fig. 4, showing the mean continuous rating across all participants. Before computing the means, the CR raw data were standardized per trial pair by subtracting the minimum rating and dividing by the rating range. The mean values of the continuous ratings (MCA_{FIL} = 4.0, MCA_{OPT} = 1.5) also differ significantly; $t(15) = 3.6708$, $p < 0.001$. Participants were consistent when rating the perceived motion mismatch continuously (Cronbach's alpha, mean: 0.83, std: 0.07). As shown in Table 3, from the 16 participants only two did not pass the statistical test for consistency (Cronbach's Alpha < 0.7) (Hair, Black, Babin, & Anderson, 2009). This result is in line with previous findings in which the same method was used to determine MCA perceived quality (Cleij et al., 2015).

4.2. Rating results per manoeuvre

Differences between MCAs rating on specific manoeuvres were analysed by comparing the mean continuous rating of the two MCAs per manoeuvre. The continuous rating for manoeuvres 'InitAcc' and 'FinalDec' was not recorded fully and was

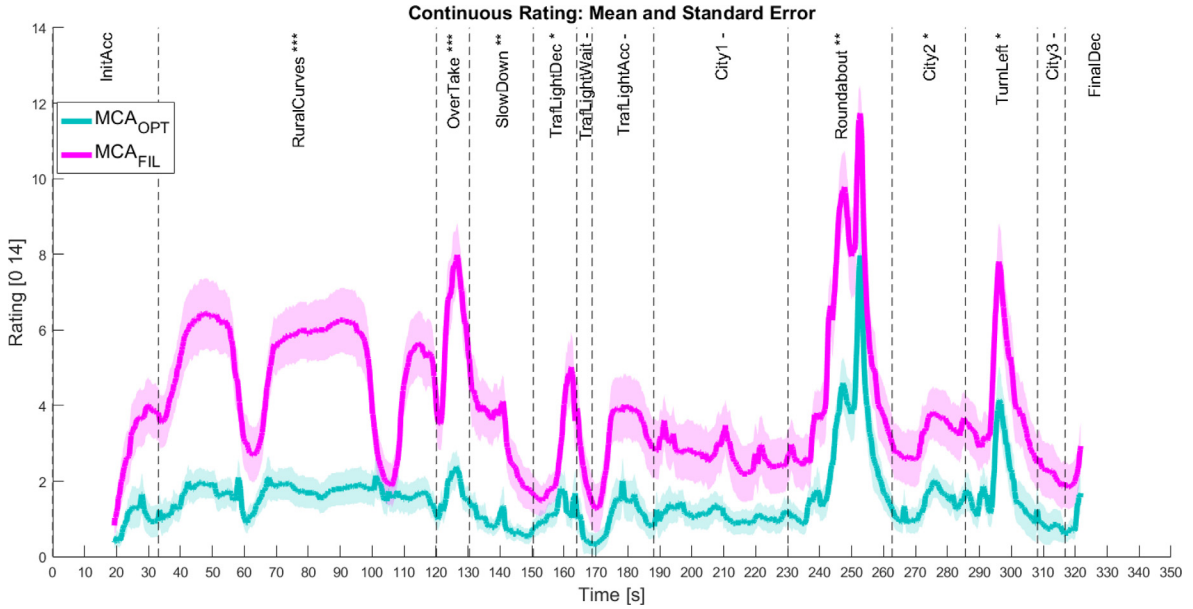

Fig. 4. Mean continuous rating (line) and standard error (shaded area). Significance of the difference between MCAs is indicated per manoeuvre with ***(p-adjusted < 0.001), **(p-adjusted < 0.01), *(p < 0.05) or – (p-adjusted > 0.05). No symbol indicates no statistical test is performed.

Table 3
Consistency test (Cronbach's Alpha) for participants' continuous rating.

Participant	Cronbach's alpha
0	0.894
1	0.828
2	0.883
3	0.868
8	0.822
9	0.897
10	0.884
11	0.843
12	0.888
13	0.84
14	0.683[a]
15	0.875
16	0.671[a]
17	0.886
18	0.727
19	0.854

[a] Two participants did not reach 0.7.

therefore excluded from the analysis. To control for the false discovery rate of multiple comparisons the Benjamini-Hochberg correction was applied to all corresponding p-values before testing for significance. The resulting test statistics and the significantly different means per MCA are shown in Table 4.

4.3. Comparison between rating and cueing errors

To determine which motion cueing errors were responsible for the measured perceived mismatch the data is split in different Manoeuvre Sets. For these sets only the manoeuvres that were rated significantly different between the two MCAs are used.

- Set Longitudinal (X): 'SlowDown', 'TrafLightDec'
- Set Lateral (Y): 'RuralCurves', 'OverTake', 'City2'
- Set Combination (XY): 'Roundabout', 'TurnLeft'

The mean of the continuous ratings over all participants was compared to the errors in 9 motion channels: linear accelerations in x, y and z direction, rotational rate and angle in roll, pitch and yaw. In Table 5 the correlations (Pearson correlation coefficient r) between MCA continuous rating and the absolute error in different motion channels is shown per Manoeuvre Set. Correlations also occur between some of the motion channels themselves, such as yaw and lateral acceleration, which can make it difficult to determine exactly which error is rated. Nonetheless the correlation together with the maximum size of the absolute error (ε_{max}) can give a good indication of whether a certain rating is likely to be caused by the error in a specific motion channel. The boldface values in Table 5 show the highest correlation coefficients and corresponding maximum error for each column of the table.

From Table 5 one can see that the mean continuous rating correlates with errors in different motion channels for each MCA. For the longitudinal manoeuvres the MCA_{OPT} rating correlates best with the pitch angle error, while the MCA_{FIL} rating correlates best with the longitudinal acceleration error. For the lateral manoeuvres a similar observation can be made; here the MCA_{OPT} rating correlates best with the roll angle error, while the MCA_{FIL} rating correlates best with the lateral acceler-

Table 4
Test statistics for the differences in mean continuous rating per manoeuvre.

Manoeuvre	Test statistic (means MCA_{FIL}/MCA_{OPT})
RuralCurves***	$t = 4.3771$ (5.1/1.7)
OverTake***	$z = 3.9762$ (6.1/1.7)
SlowDown**	$t = 3.4159$ (3.2/0.9)
TrafLightDec*	$t = 2.8780$ (2.7/1.2)
TrafLightWait	$z = 1.7721$
TrafLightAcc	$z = 2.0919$
City1	$z = 1.5270$
Roundabout**	$t = 3.3070$ (5.5/2.6)
City2**	$t = 2.5093$ (3.2/1.4)
TurnLeft*	$t = 2.8131$ (4.1/1.9)
City3	$z = 0.9526$

***p-adjusted < 0.001, **p-adjusted < 0.01, *p-adjusted < 0.05 and otherwise p-adjusted > 0.05.

Table 5
Correlation coefficients between continuous rating and absolute motion errors.

Set	Longitudinal				Lateral				Combination			
MCA	MCA_{OPT}		MCA_{FIL}		MCA_{OPT}		MCA_{FIL}		MCA_{OPT}		MCA_{FIL}	
Correlation/error	r	ε_{max}	r	ε_{max}	r	ε_{max}	r	ε_{max}	r	ε_{max}	r	ε_{max}
Longitudinal Acc	0.84	0.09	**0.86**	**2.22**	0.60	0.10	0.43	0.74	0.70	0.82	0.45	1.92
Lateral Acc	0.86	0.07	0.48	0.29	0.62	0.23	**0.92**	**1.41**	0.92	1.62	**0.90**	**3.61**
Vertical Acc	0.87	0.13	0.72	0.02	0.90	0.08	0.79	0.03	0.86	0.26	0.84	0.16
Roll Rate	0.68	0.25	0.23	0.53	0.61	1.98	0.38	1.58	**0.93**	**6.27**	0.70	1.53
Pitch Rate	0.78	1.95	0.72	0.70	0.68	1.05	0.45	0.31	0.85	4.27	0.57	0.79
Yaw Rate	0.85	0.16	0.43	1.12	0.69	3.20	0.81	5.06	0.84	9.42	0.88	26.10
Roll Angle	0.65	0.96	0.26	0.86	**0.91**	**8.39**	0.88	3.23	0.80	14.16	0.85	4.88
Pitch Angle	**0.92**	**7.55**	0.82	2.60	0.50	5.43	0.42	1.36	0.60	6.47	0.44	3.09
Yaw Angle	0.81	17.79	0.71	13.33	0.87	18.50	0.72	43.00	0.46	58.83	0.55	77.90

Boldface values indicate highest correlation coefficients and corresponding maximum error for each column of the table.

ation error. It is also notable that the maximum pitch angle error is relatively high for the MCA_{OPT}, but no clear correlation between this error and the rating is found. For the manoeuvres with both strong longitudinal and lateral acceleration errors the MCA_{OPT} correlates best with the roll rate error, while the MCA_{FIL} correlates best with the lateral acceleration error. Additionally a strong correlation between lateral acceleration error and the rating for the MCA_{OPT} is also found.

Overall the rating for the MCA_{FIL} correlates best with the linear acceleration error, while the rating for the MCA_{OPT} correlates best with the rotational error.

4.4. Motion cueing mechanisms

The MCAs utilize very different approaches to deal with the limited motion space of the simulator. While these mechanisms are explicitly programmed for the MCA_{FIL}, the mechanisms used by MCA_{OPT} are only revealed when analysing the resulting optimized simulator motions. In the following paragraphs these different mechanisms are described.

Global scaling of the vehicle motions is an often used mechanism to guarantee that the simulator motions stay within the simulator motion space, while the visual and vestibular motions remain coherent. The MCA_{FIL} relies to a large extent on a global scaling of the vehicle motion, resulting in significantly reduced motion strengths. Because the MCA_{OPT} uses an optimization at each time step, motion scaling is only applied at those time steps where this is required (i.e., local scaling), resulting in virtually no global scaling.

Washout of the simulator motions is an often used mechanism to keep the simulator within its motion limits. This mechanism returns the simulator to its neutral position, such that simulator excursions in all simulator degrees of freedom are still possible. This mechanism is used by the MCA_{FIL} via high pass filtering of the accelerations that are produced via the simulator's linear rail and hexapod translations. While the MCA_{OPT} has a similar mechanism implemented, currently this was not used (as $Q = 0$ in Eq. (1)).

Tilt-coordination is an often used mechanism to simulate sustained linear accelerations while keeping the simulator within the simulator workspace. The simulator is slowly tilted such that a component of the gravitational acceleration can be used to simulate the desired longitudinal or lateral acceleration. This mechanism is explicitly implemented in the MCA_{FIL} where filters are used to obtain the low frequent vehicle accelerations that can be simulated with tilt-coordination. Even though this mechanism is not explicitly implemented in the MCA_{OPT}, the optimization can result in similar behaviour, trading tilt rate errors for improved performance in linear acceleration simulation. From Fig. 5 it can be seen that this trade-off results in much higher tilt rates for MCA_{OPT} than for MCA_{FIL}. The perceptual threshold of 3°/s (Groen & Bles, 2004), indicated with the striped black line, is only reached during the manoeuvres 'Roundabout' and 'TurnLeft'. The effect of using tilt-coordination for both MCAs is clearly visible in Fig. 8 where the green line indicates the acceleration in the driver reference frame that is produced via tilt-coordination.

Prepositioning is a mechanism used by the MCA_{OPT} to extend the motion space of the simulator. Knowing future motions, the MCA_{OPT} positions the simulator in such a way that the available excursion for this future motion is maximized. Instead of moving the simulator to the neutral position as done with the washout mechanism, prepositioning results in moving the simulator to extreme positions of the simulator. For example, several seconds before the manoeuvre 'OverTake', the hexapod is slowly moved to a large lateral offset to the right (~1.1 m) (MCA_{OPT} at $t = 5.5$[s], Fig. 6). This prepositioning doubles the available leftward excursion needed for the linear accelerations of the future motion.

A similar prepositioning strategy can be identified for the manoeuvre 'Roundabout'. Here, the available clockwise yaw excursion of the hexapod is maximized by very slowly prepositioning the hexapod to a counterclockwise yaw angle of ~21° (MCA_{OPT} at $t = 120$[s], Fig. 7 top) before entering the roundabout. In this case the mechanism starts about 110 s before the start of the roundabout manoeuvre. For the manoeuvre 'LeftTurn', the available yaw excursion is maximized about 10 s before the turn starts (MCA_{OPT} at $t = 161$[s], Fig. 7 top). Here the algorithm traded an error in yaw rate just before the turn (MCA_{OPT} between $t = 161$[s] and $t = 171$[s], Fig. 7 bottom) for additional yaw excursion possibilities while driving through the turn (between $t = 171$[s] and $t = 179$[s]).

Velocity buffering, which is only utilized by the MCA_{OPT}, is the final mechanism that will be discussed here. In velocity buffering the simulator's velocity is utilized to maximize the simulator's future acceleration capabilities. It can be interpreted as the velocity equivalent of the prepositioning mechanism. By giving the simulator a velocity in one direction, the duration for which the simulator can then accelerate in the opposite direction is increased. In the experiment, velocity buffering was most clearly observed during manoeuvres 'InitAcc' and 'TrafLightWait'. As shown in the top plot of Fig. 8, the MCA_{FIL} did not result in simulator motion during the vehicle's standstill (between $t = 0$[s] and $t = 15.5$[s] and between $t = 33$[s] and $t = 38$[s]), but the MCA_{OPT} generated a backwards simulator motion via the linear rail (blue[1] line) and hexapod translation (red line) during the vehicle's standstill. At the same time the simulator pitch angle was slowly increased (green line) to counteract the generated backward motion, resulting in a linear acceleration (black line) of zero in the driver frame of reference. The pitch rate was constant at 0.9°/s for the manoeuvre 'TrafLightWait' and increased from 0 to 1.5°/s for the manoeuvre 'InitAcc'. Upon accelerating (at $t = 15.5$[s] and $t = 38$[s]), the initial forward vehicle acceleration was simulated by first *slowing down* the backwards motion (green and red lines) before the simulator obtained forward velocity, effectively extending the duration at which the forward acceleration could be sustained. This mechanism was mainly used to improve the high frequent initial acceleration

[1] For interpretation of color in Figs. 7 and 8, the reader is referred to the web version of this article.

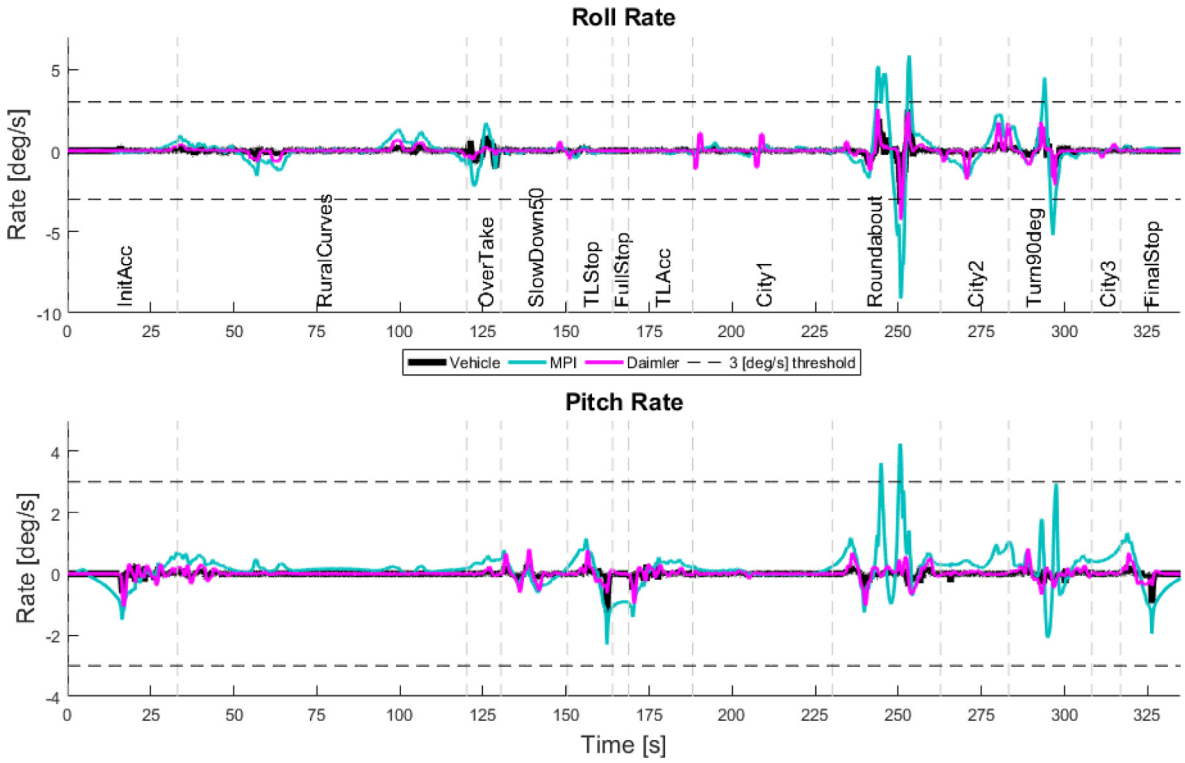

Fig. 5. Tilt rates in head frame of reference for all manoeuvres and both MCAs.

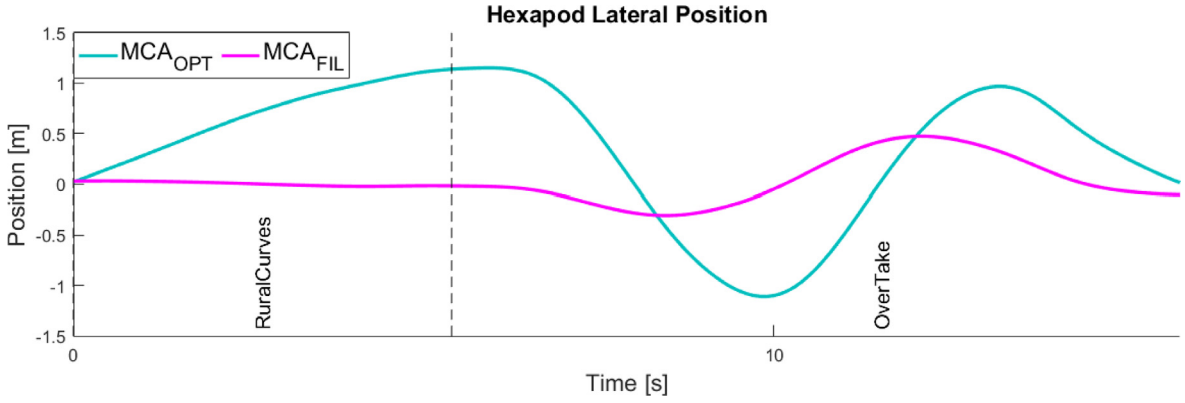

Fig. 6. Hexapod lateral position for the end of the manoeuvre 'RuralCurves' and the manoeuvre 'OverTake' for both MCAs.

cue provided by the hexapod translation (during both manoeuvres) and the linear rail (mainly during manoeuvre 'InitAcc'). Effective velocity buffering requires accurate knowledge on future accelerations in order not to exceed actuator position limits.

4.5. Linear acceleration simulation in the Daimler simulator

There are multiple ways in which the Daimler simulator, consisting of a linear rail and a hexapod, can be used to generate linear acceleration in the driver frame of reference. Investigating the sources of the linear accelerations resulting from either MCA gives a better insight in how the different cueing mechanisms and the capabilities of the Daimler simulator are exploited by these MCAs. Table 6 shows the contributions of the different sources of acceleration as a percentage of the required vehicle acceleration (first value) and as a percentage of the generated total simulator acceleration (second value) in the driver frame of reference. As the MCA_{OPT} results in very small acceleration errors (i.e. vehicle and simulator accelerations in the driver frame of reference are almost equal), the two percentages are very similar for this MCA.

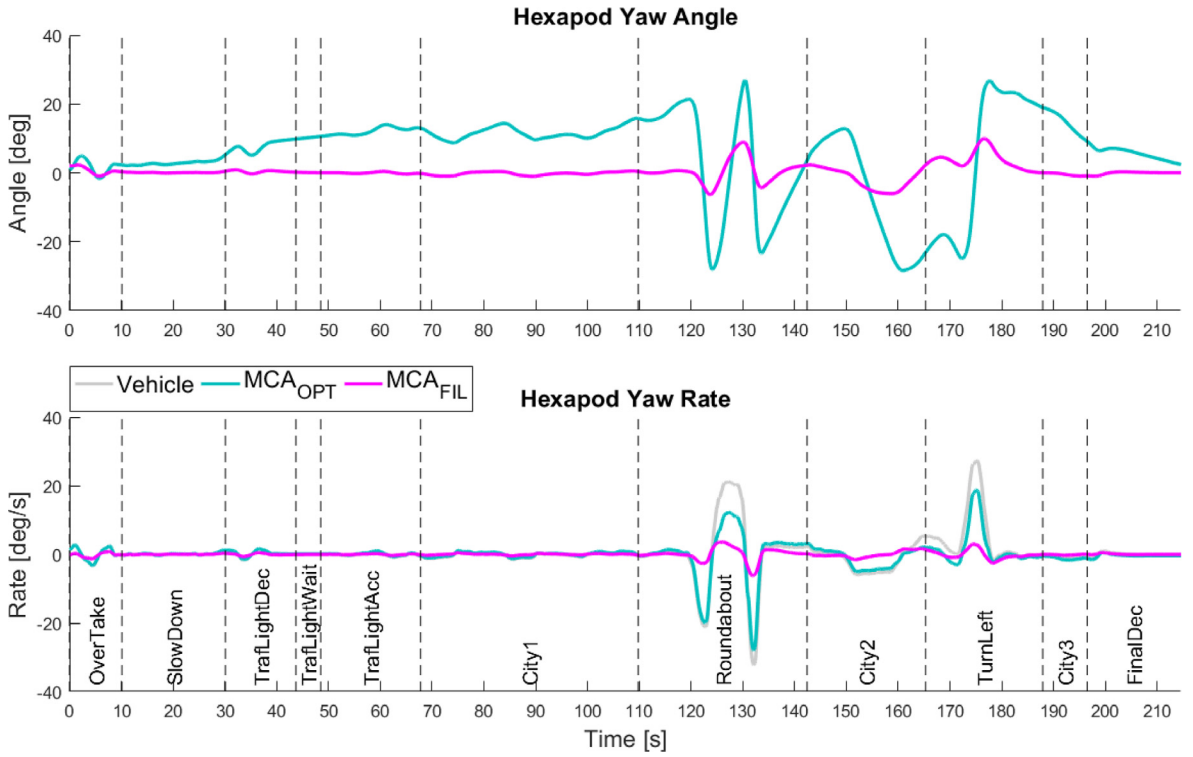

Fig. 7. Yaw angle (top) and yaw rate (bottom) during several manoeuvres for both MCAs.

Table 6
Contributions of different acceleration sources to the longitudinal and lateral acceleration in the driver frame of reference.

Acceleration	Longitudinal (X)		Lateral (Y)	
MCA	MCA_{OPT}	MCA_{FIL}	MCA_{OPT}	MCA_{FIL}
Gravitational acceleration (GA)	99.5%/100%	19.3%/80.3%	82.0%/87.6%	24.2%/90.7%
Linear rail acceleration (LRA)	41.3%/41.5%	12.4%/51.4%	7.8%/8.3%	0.2%/0.8%
Hexapod X acceleration (HXA)	17.1%/17.2%	2.4%/9.9%	2.5%/2.7%	0%/0.2%
Hexapod Y acceleration (HYA)	4.3%/4.3%	0.2%/0.9%	17.6%/18.8%	4.6%/17.4%
Hexapod Z acceleration (HZA)	0.2%/0.2%	0.0%/0.0%	0.1%/0.1%	0.0%0.0%
Hexapod roll acceleration (HRA)	0.8%/0.8%	0.1%/0.3%	2.5%/2.7%	1.1%/4.1%
Hexapod pitch acceleration (HPA)	2.4%/2.4%	0.7%/2.8%	0.5%/0.5%	0.0%/0.0%

The gravitational acceleration contributes to both linear and longitudinal acceleration in the driver frame of reference via the tilt-coordination mechanism. When the hexapod yaw angle is zero, an acceleration of the hexapod over the linear rail simulates longitudinal acceleration in the driver frame of reference. When the hexapod yaw angle differs from zero, this source can also produce lateral acceleration in the driver frame of reference. The hexapod translation capabilities can also be used to simulate short duration longitudinal and lateral linear accelerations in the driver frame of reference. In combination with a hexapod tilt angle, translation accelerations in one direction can contribute to the linear acceleration in a different direction in the driver frame of reference. Finally, because the hexapod coordinate system is positioned 1.6 meter below the driver's eye point, also the roll and pitch acceleration of the hexapod cause small linear accelerations in the driver frame of reference.

As can be derived from Table 6, the sum of the contributions of all these sources is not necessarily 100%. This can be explained by the occurrence of counter acting accelerations produced by different sources resulting in a simulator acceleration of zero in the driver frame of reference. As shown in Fig. 8 (top) this occurs, for example, during prepositioning (from $t = 0$[s] to $t = 15.5$[s]) and velocity buffering (from $t = 33$[s] to $t = 38$[s]) where the linear rail (blue line) and hexapod (red line) accelerations counter act the gravitational acceleration (green line). The total acceleration produced by the individual sources is thus higher than the resulting acceleration in the driver frame of reference.

Both the MCA_{FIL} as well as the MCA_{OPT} use the gravitational acceleration as their main source for simulating both longitudinal and lateral acceleration in the driver frame of reference. However, the angular rates produced by the MCA_{OPT} are much larger than those produced by the MCA_{FIL} (means of 0.47 and 0.39°/s versus 0.14 and 0.09°/s in roll and pitch respec-

tively). Table 6 shows that this source is responsible for 100% of the total longitudinal simulator acceleration in the drivers reference frame when using the MCA_{OPT}. To keep the corresponding tilt rate low, the tilt angle is slowly increased before the motion starts as can be seen from the green line between for example $t = 30$[s] and $t = 33$[s] in the top plot of Fig. 9. At the same time the resulting false rotational cue is minimized by the hexapod (red line) and linear rail (blue line) accelerations in opposite direction. The MCA_{FIL} also counter acts the excess gravitational acceleration from tilt-coordination with linear rail accelerations, but does so only at the end of the manoeuvre as can be seen around $t = 15$[s] and $t = 22$[s] in the bottom plot of Fig. 9.

The MCA_{FIL} is designed to use tilt-coordination for sustained accelerations, while using the linear rail and hexapod translations for high frequent motions. This is clearly visible in Fig. 9 (bottom) during the manoeuvre 'SlowDown' where the linear rail (blue line) is used for the initial and final high frequent part of the motion while the low frequent part of the motion is produced by the gravitational acceleration (green line). In Fig. 10 (bottom) instead of the linear rail, the hexapod lateral acceleration (yellow line) is used for the very low amplitude high frequent part of the motion throughout the curves. Even though the MCA_{OPT} does not explicitly implement such a division in the frequency domain, the optimization algorithm comes up with a very similar solution. This effect is especially well visible in Fig. 10 (top), where all high frequent variations of the lateral accelerations are generated via hexapod lateral acceleration (yellow line). The benefit of not implementing a hard division for high and low frequencies explicitly is that the linear rail can also be used for low frequent motions as seen clearly by the blue line in Fig. 9 (top) during the manoeuvre 'TrafLightDec'.

Table 6 also shows an interesting difference between the usage of the linear rail accelerations as a source for both lateral and longitudinal acceleration in the driver reference frame. In the currently used Daimler simulator configuration, the linear rail can be used for longitudinal acceleration when the hexapod yaw angle is equal to zero. Table 6 shows that both MCAs produce around half of the longitudinal simulator motions in the driver reference frame using this source. Due to the use of linear rail accelerations for low frequent motions as well as the use of the prepositioning and velocity buffering mechanisms, the linear rail accelerations account for a much larger part of the total vehicle acceleration when using the MCA_{OPT} than when using the MCA_{FIL}.

When applying a yaw angle to the hexapod, the linear rail acceleration can also be used to simulate lateral vehicle acceleration which, as Table 6 indicates, is only used by the MCA_{OPT}, where 7.8% of the lateral vehicle acceleration is produced in this way. As shown in Fig. 11, the MCA_{OPT} uses this mechanism effectively during the roundabout manoeuvre where the linear rail acceleration (blue line) contributes maximally at $t = 15$[s] with 0.5 m/s^2 to the lateral acceleration in the drivers reference frame. Since the yaw angle of the hexapod is always smaller than 90°, using this mechanism for lateral acceleration

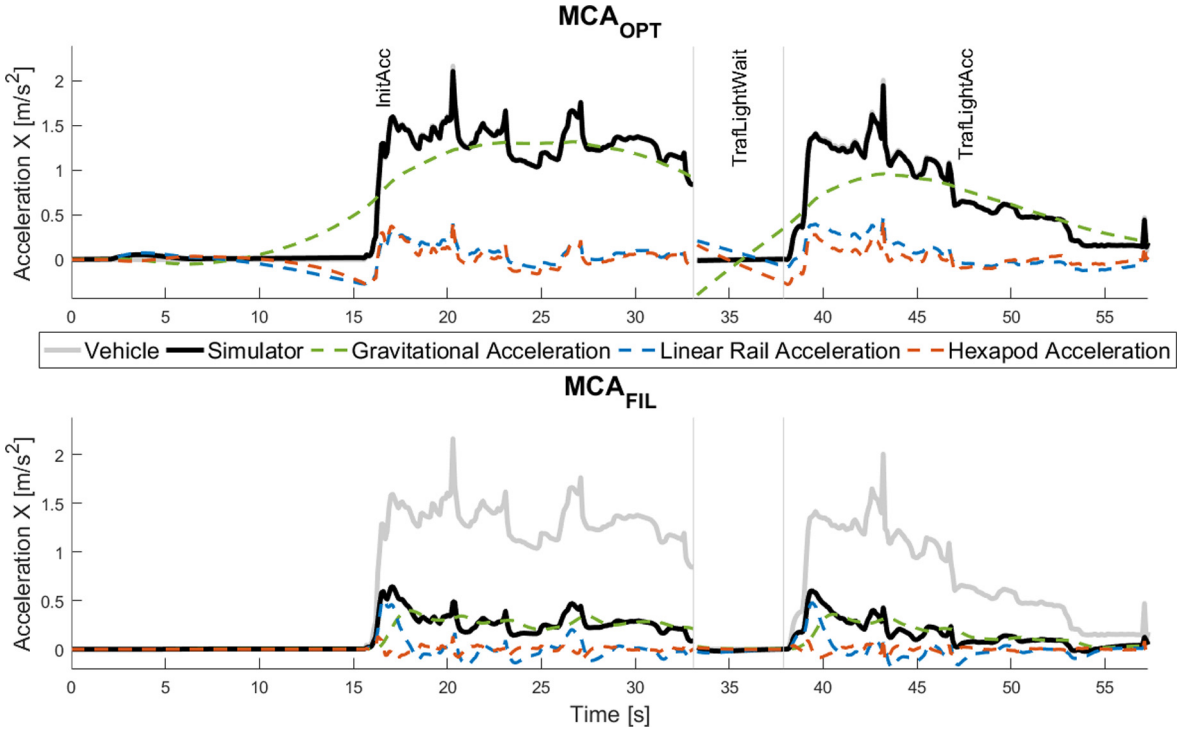

Fig. 8. Contributions of different acceleration sources to the longitudinal acceleration in the driver frame of reference for manoeuvres 'InitAcc', 'TrafLightWait' and 'TrafLightAcc' using the MCA_{OPT} (top) and the MCA_{FIL} (bottom).

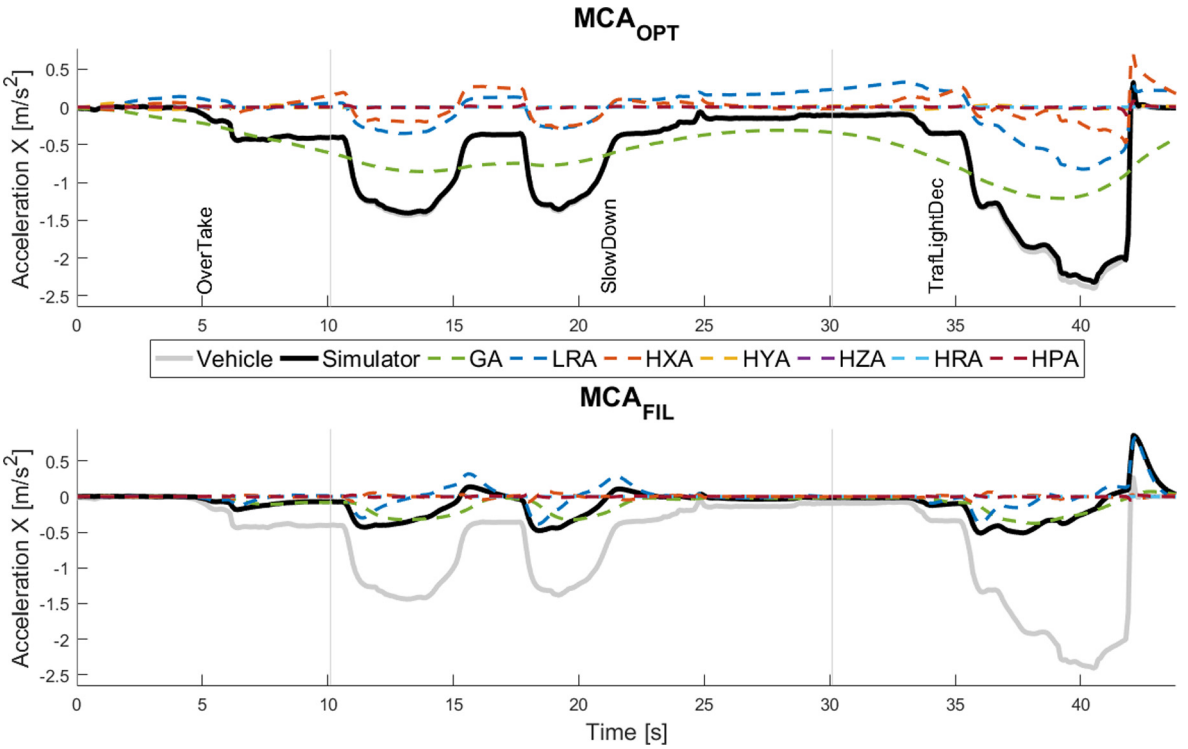

Fig. 9. Contributions of different acceleration sources to the longitudinal acceleration in the driver frame of reference for the manoeuvres 'OverTake', 'SlowDown' and 'TrafLightDec' using the MCA_{OPT} (top) and the MCA_{FIL} (bottom).

creates an additional parasitic longitudinal acceleration. Fig. 12 between $t = 14$[s] and $t = 17$[s] shows that the MCA_{OPT} uses pitch tilt-coordination (green line[2]) to counteract the parasitic longitudinal acceleration (blue line).

5. Discussion

The perceived motion mismatch for the MCA_{FIL} and MCA_{OPT} were rated using two measurement methods, both showing a significantly larger perceived motion mismatch when using the MCA_{FIL} than when using the MCA_{OPT}. This indicates that the MCA_{OPT} indeed has the potential to further improve motion cueing in simulators such as the DDS. The rating methods both showed very similar ratios between the MCA_{FIL} and the MCA_{OPT} (OR: 2.32, CR: 2.67), implying that the mean of the continuous rating was a good indicator for the overall rating of the complete drive. The consistency of both the overall and the continuous rating between trials indicates that learning, habituation or fatigue effects did not impact these ratings significantly, and participants were able to provide consistent estimates during the whole experiment.

A more in detail analysis of the continuous rating shows that the difference between MCAs is mainly caused by the manoeuvres 'Overtake' and 'RuralCurves', where the largest significant difference between the mean ratings was found. It is especially surprising that during the 'RuralCurves' manoeuvre, where the MCA_{FIL} simply scales down the motion, such a large difference between MCAs is found. The often used mechanism of scaling, here with a factor of 0.3 during the 'RuralCurves' manoeuvre, can thus have a larger impact on the perceived mismatch in motion simulation than often assumed. The continuous rating also showed that for both MCAs the manoeuvre 'Roundabout' is rated as the worst of all manoeuvres presented during the drive. It is notable that even with full knowledge of the future motions the MCA_{OPT} still resulted in a strong perceived motion mismatch during this manoeuvre. However, also here an optimization-based approach has the potential to significantly improve motion cueing compared to a filter-based approach. In this study, the manoeuvres resulting in large lateral accelerations showed the largest difference between MCAs. It should be noted that better results for these manoeuvres could likely be obtained by aligning the car's lateral axis with the simulator's linear axis.

The extensive use of global scaling mechanism by the MCA_{FIL} and the lack of any global scaling in the MCA_{OPT} is the largest difference between the two MCAs. This resulted in larger linear acceleration errors for the MCA_{FIL} than for the MCA_{OPT}. Instead, the MCA_{OPT} made much more use of tilt-coordination mechanism, resulting in higher rotation errors. The effect of

[2] For interpretation of color in Fig. 11, the reader is referred to the web version of this article.

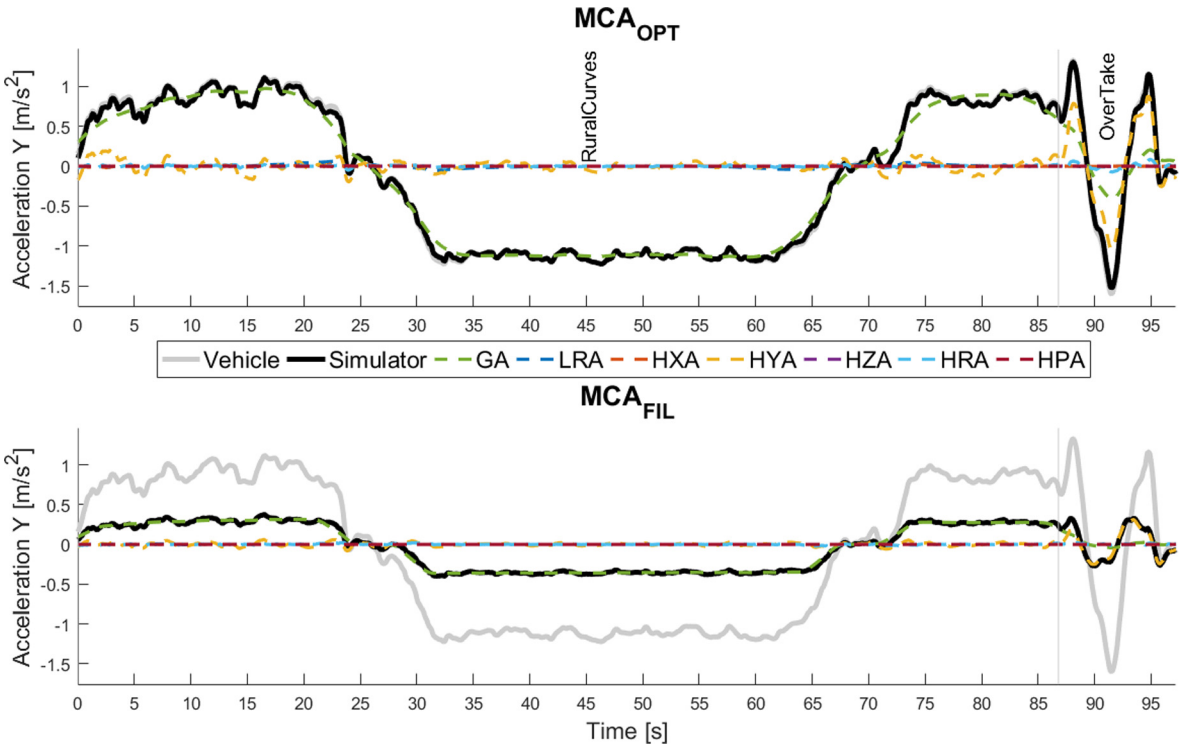

Fig. 10. Contributions of different acceleration mechanisms to the lateral acceleration in the driver's coordinate system for the manoeuvres 'RuralCurves' and 'OverTake' using the MCA_{OPT} (top) and the MCA_{FIL} (bottom).

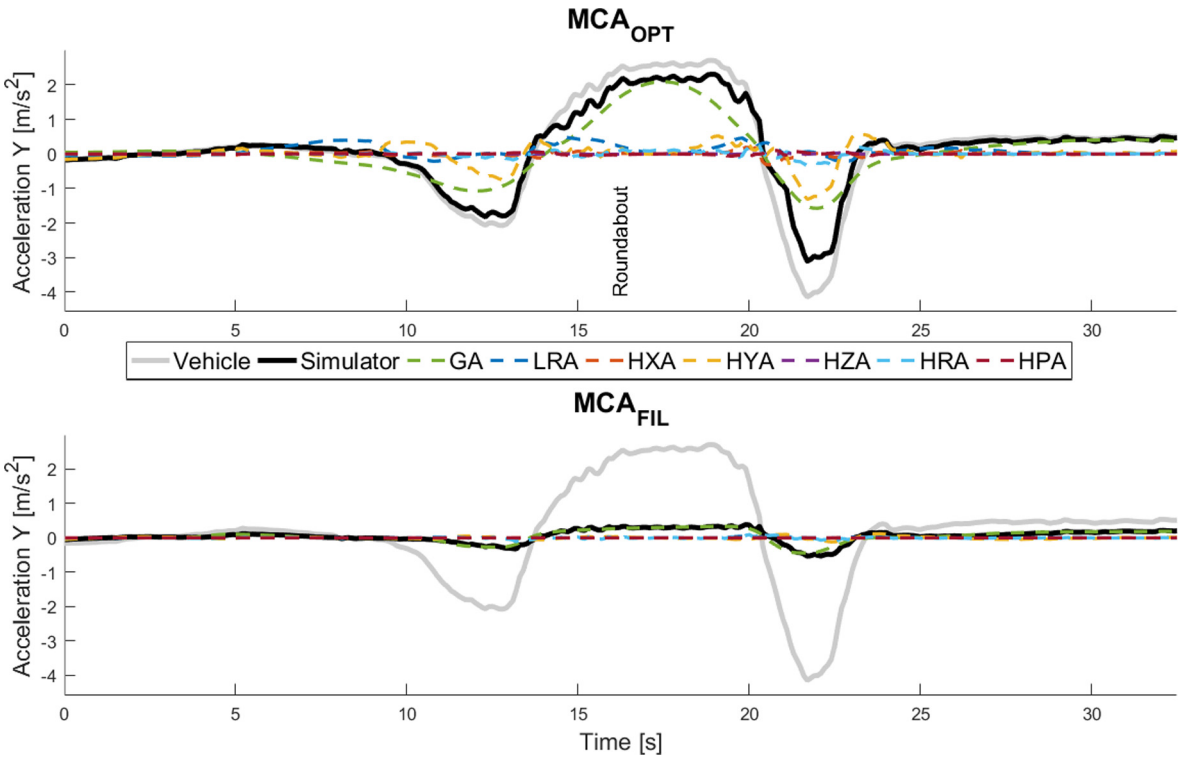

Fig. 11. Contributions of different acceleration mechanisms to the lateral acceleration in the driver's coordinate system for the manoeuvre 'Roundabout' using the MCA_{OPT} (top) and the MCA_{FIL} (bottom).

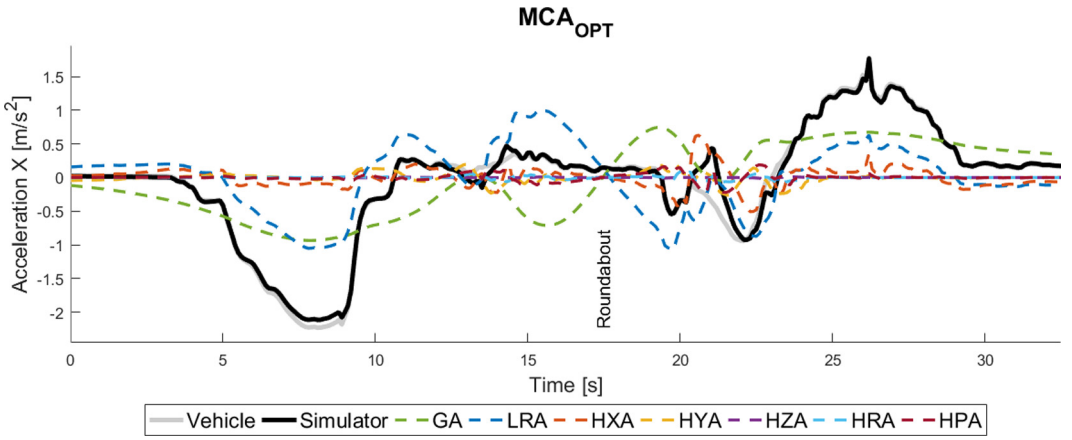

Fig. 12. Contributions of different acceleration mechanisms to the longitudinal acceleration in the driver's coordinate system for the manoeuvre 'Roundabout' using the MCA_{OPT}.

these choices is also visible in the continuous rating results. The MCA_{OPT} rating showed a higher correlation to rotation errors, while the MCA_{FIL} showed a higher correlation to the errors in linear accelerations. These correlations indicate that both error types were perceived by the participants. The mean continuous rating, however, was significantly higher for the MCA_{FIL} than for the MCA_{OPT}. This indicates that, a higher tilt rate that results in false rotational cues, would have been more acceptable than the degree of global scaling as done by the MCA_{FIL} to avoid these false cues.

One advantage of global scaling is that the resulting simulator motions are less strong, but still in coherence with the desired vehicle motions. Currently the MCA_{OPT} managed to minimize the acceleration errors so well, that low coherence did not seem to be an issue during most of the drive. If the acceleration errors increase, for example when using a limited prediction horizon, unpredictable scaling of the linear accelerations might become a problem. In this case global scaling could also become necessary for the MCA_{OPT}.

The correlation analysis also indicates that the participants rated rotational angles instead of rotational rates during the lateral and longitudinal manoeuvre sets. This finding indicates that not only the tilt rate, but also a tilt angle can be perceived as a false cue and should be taken into account when optimizing a motion cueing algorithm.

During the 'TrafLightWait' manoeuvre there were no vehicle motions. The MCA_{OPT}, however, uses this time for velocity buffering and prepositioning which results in significant simulator motion. The corresponding continuous rating of the MCA_{OPT} for this manoeuvre does not show a significant increase in perceived mismatch, indicating that this motion was not perceived or did not bother the participants. This could be explained by the tilt rate of 0.9°/s, which is often found to be below the human threshold for rotational rate, and a resulting acceleration of zero. In practice, however, simulator motion can often be felt through the generation of parasitic rumble-like motions. In the Daimler simulator special attention was given in the design for this purpose, resulting in very smooth simulator motions. Using simulator motions for prepositioning or velocity buffering during standstill is therefore only recommended for high quality motion simulators. For both these mechanisms knowledge of the future vehicle trajectory is necessary. Reducing the prediction horizon of an MPC-based algorithm will therefore also reduce the possibilities of using these mechanisms.

The trade-off made by the MCA_{OPT} to reduce the yaw rate before the 'LeftTurn' manoeuvre in order to increase the available yaw rate while driving through the turn could be responsible for the slight increase in continuous rating at this point. During the 'LeftTurn' manoeuvre continuous rating also shows a clear perceived motion mismatch. Further research could determine if such trade-offs are beneficial and the MPC cost function should be adjusted correspondingly.

For the manoeuvres 'City1' and 'City3' no significant difference between the MCAs was found. The maximum vehicle acceleration during these manoeuvres was 0.36 in lateral direction, compared to 1.45 m/s^2 during manoeuvre 'City2', where significant differences between MCAs were found. The high scaling factor of the MCA_{FIL} thus does not seem to reduce the perceived motion mismatch significantly for accelerations below 0.36. It is likely that the resulting absolute errors were close to the human perceptual threshold for lateral inertial acceleration and were thus not perceived as incoherent with the visual motions.

6. Conclusions

The results of the experiment lead to the following conclusions:

- The results show that participants were able to rate the perceived mismatch consistently over the various repetitions. This holds for both the overall rating (Fig. 3 right plot) as for the continuous rating (Table 3).

- The rating results (Fig. 3 right plot and Fig. 4) show that optimization-based cueing algorithms such as MCA_{OPT} indeed have the potential to improve motion cueing compared to filter-based approaches such as MCA_{FIL}.
- The continuous rating (Fig. 4) shows that avoiding global scaling of the vehicle motions, as can be done with optimization-based cueing algorithms, has a large impact on the perceived motion mismatch especially during rural road simulations. The rating also showed that simulating a roundabout manoeuvre is difficult even for optimization-based approaches such as MCA_{OPT}. However, a significant improvement can still be made compared to filter-based-approaches such as MCA_{FIL}.
- The comparison of the continuous rating with the motion errors (Table 5) indicates that a certain amount of detectable rotation errors could be preferred over large scaling errors.
- Several mechanisms were identified that contributed to the differences observed between the two algorithms: global scaling, washout, tilt-coordination, prepositioning and velocity buffering. Additionally an overview was given (Table 6) of how the two MCAs used the different sources of linear acceleration in the Daimler Driving Simulator.

It should be noted that the two MCAs are very different algorithms, each with their own characteristics.

This study is therefore not to be considered as a competitive comparison between MCA alternatives, but rather as an attempt to gain insight in the potential that an optimization-based approach has to offer. The results show that there exists a potential to further improve the quality of the motion simulation with optimization-based methods, deserving of further research.

Regarding the rating method, the results show that the rating method provides reliable and repeatable results within and between participants, which further confirms the reliability and utility of the method. Ongoing research investigates the dynamics and limitations of the rating behaviour.

In future experiments it could be investigated how the quality of the MCA_{OPT} degrades if the prediction horizon is decreased (i.e., no longer using trajectory-based optimization) or if the prediction is imperfect (i.e., no longer using the pre-recorded trajectory but a predicted trajectory). Also, it could be studied how the objective function can be adapted to further improve the quality of the MCA_{OPT}. Finally, it would be interesting to investigate whether the tuning of the MCA_{FIL} can be further improved based on the more detailed analysis of the results presented in this paper.

References

Anderson, J. (2013). A general-purpose software framework for dynamic optimization. *PhD thesis*. Arenberg Doctoral School, KU Leuven.

Beghi, A., Bruschetta, M., & Maran, F. (2012). A real time implementation of MPC based Motion Cueing strategy for driving simulators. In *51st IEEE conference on decision and control* (pp. 6340–6345), Maui, HI, USA.

Cleij, D., Venrooij, J., Pretto, P., Pool, D. M., Mulder, M. & Bülthoff, H. H. (2015). Continuous rating of perceived visual-inertial motion incoherence during driving simulation. In *DSC 2015 Europe: Driving simulation conference & exhibition* (pp. 191–198), Tübingen, Germany.

Garrett, N. J. I., & Best, M. C. (2010). Driving simulator motion cueing algorithms – a survey of the state of the art. In *Proceedings of the 10th international symposium on Advanced Vehicle Control (AVEC)* (pp. 183–188), Loughborough, UK.

Garrett, N. J. I., & Best, M. C. (2013). Model predictive driving simulator motion cueing algorithm with actuator-based constraints. *Vehicle System Dynamics, 51*(8), 1151–1172.

Groen, E. L., & Bles, W. (2004). How to use body tilt for the simulation of linear self motion. *Journal of Vestibular Research, 14*(5), 375–385.

Hair, J. F., Black, W. C., Babin, B. J., & Anderson, R. E. (2009). *Multivariate data analysis* (7th ed.). Prentice Hall.

Katliar, M., De Winkel, K. N., Venrooij, J., Pretto, P. & Bülthoff, H. H. (2015). Impact of MPC prediction horizon on motion cueing fidelity. In *DSC 2015 Europe: Driving simulation conference & exhibition* (pp. 219–222), Tübingen, Germany.

Maran, F., Bruschetta, M., Beghi, A. & Minen, D. (2015). Improvement of an MPC-based motion cueing algorithm with time-varying prediction and driver behaviour estimation. In *DSC 2015 Europe: Driving simulation conference & exhibition* (183–190), Tübingen, Germany.

Mayrhofer, M., Langwallner, B., Tischer, W., Schlüsselberger, R., Bles, W. & Wentink, M. (2007). An innovative optimal control approach for the next generation motion platform DESDEMONA. In *AIAA modeling and simulation technologies conference* (pp. 1–14), Hilton Head, SC, USA.

Pretto, P., Venrooij, J., Nesti, A. & Bülthoff, H. H. (2015). Perception-based motion cueing: A cybernetics approach to motion simulation. In S. -W. Lee (Ed.), *Recent progress in brain and cognitive engineering* (pp. 131–152). Springer, Dordrecht, The Netherlands.

Rawlings J. B., Mayne, D. Q. (2015). *Model predictive ConTrol: Theory and design* (5th ed.). Nob Hill Pub.

Venrooij, J., Pretto, P., Katliar, M., Nooij, S. A. E., Nesti, A., Lächele, M., de Winkel, K.N., Cleij, D. & Bülthoff, H. H. (2015). Perception-based motion cueing: validation in driving simulation. In *DSC 2015 Europe: Driving simulation conference & exhibition* (pp. 153–161), Tübingen, Germany.

Wächter, A., & Biegler, L. T. (2006). On the implementation of a primal-dual interior point filter line search algorithm for large-scale nonlinear programming. *Mathematical Programming, 106*(1), 25–57.

Zeeb, E. (2012). Daimler's new full-scale, high-dynamic driving simulator - A technical overview. In *DSC 2010: Driving simulation conference 2010* (pp. 157–165), Paris, France.